# Interaction of $M^{3+}$ lanthanide cations with amide, urea, thioamide and thiourea ligands: a quantum mechanical study †

PERKIN 2

**Frédéric Berny and Georges Wipff** *

*Institut de Chimie, Université Louis Pasteur, UMR CNRS 7551, 4, rue B. Pascal,*
*67 000 Strasbourg, France*

***Received (in Cambridge, UK) 11th August 2000, Accepted 13th October 2000***
***First published as an Advance Article on the web 23rd November 2000***

We report an *ab initio* quantum mechanical study on the interaction of $M^{3+}$ cations ($La^{3+}$, $Eu^{3+}$, $Yb^{3+}$) with model ligands **L** (**L** = amide, urea, thioamide and thiourea derivatives). The role of counterions and stoichiometry on ligand binding energies is investigated by a comparison of charged $\mathbf{ML}^{3+}$ complexes with the neutral $\mathbf{MCl_3L}$ and $\mathbf{MCl_3L_2}$ ones. The calculations show that all ligands display strong interactions with the cation. Trends in binding energies in $\mathbf{ML}^{3+}$ (urea > thiourea > amide > thioamide) are found to differ from those of calculated protonation energies (thiourea > urea > thioamide > amide). Adding counterions or increasing the coordination number may also modify the relative affinities. Changes in structural parameters, electron transfer and polarization effects are analysed. The calculations reveal a striking difference in the binding mode of sulfur compared to oxygen ligands, and the role of steric repulsions in the first coordination sphere, due to counterions and increased coordination number. The results are discussed in the context of modelling complexes of lanthanide and actinides.

## Introduction

The search for molecules that selectively complex lanthanides and actinides represents a challenging task from a basic point of view,[1] as well as for applications such as nuclear waste separation and minimization[2,3] or design of photoactive systems.[4–7] Generally speaking, selective complexation in solution results from the interplay of features such as desolvation of the partners (solvent stripping from the cation and the ligand), conformational change of the ligand, and solvation of the formed complex, with possible counterion effects.[8] One key requirement to form stable complexes is cation–ligand interactions that are strong enough to compete with the solvation forces. It is thus important to precisely assess the intrinsic energetic and stereochemical features of the elementary interactions between putative cations and the binding sites of the ligand. In the case of trivalent lanthanide or actinide ions, gas-phase data are not available from experiment. This led our group to undertake Quantum Mechanical (QM) computations to get information on structural, electronic and energetic features of non-covalent interactions between the metals and typical ligands. We recently reported QM *ab initio* studies on the interaction between the uranyl[9] and trivalent lanthanide cations[10,11] $M^{3+}$ with phosphoryl-containing $R_3P{=}O$ ligands (R = H, Me, Et, Ph, OMe). Ligands such as amide, pyridine, triazine or anisole derivatives were also considered.[12,13] In the series of phosphoryl ligands, we also investigated the effect of oxygen/sulfur substitution in $R_3P{=}O/R_3P{=}S$[14] and modelled the complexes with negatively charged “CYANEX-301” $R_2PS_2^-$ ligands.[15] Interest in sulfur compounds comes from the discovery of their extraction properties[16,17] and, on a theoretical basis, from the HSAB concept according to which ligands are bases and cation are acids.[18–20] The softer character of sulfur, compared to oxygen, might be a source of selectivity among the $M^{3+}$ lanthanides where the hardness decreases with the cation size (from $La^{3+}$ to $Lu^{3+}$) and for trivalent actinides which are presumably softer than lanthanides. We recently showed that, in addition to ligand basicity, electrostatic strain in the first coordination sphere is another source of ion–ligand discrimination in condensed phases.[11,15]

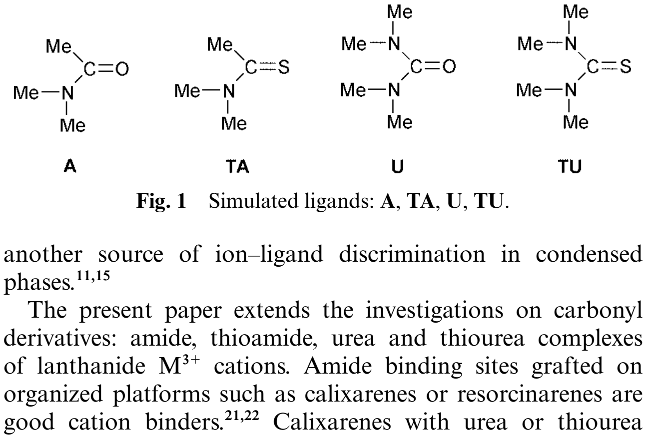
A TA U TU

Fig. 1 Simulated ligands: **A**, **TA**, **U**, **TU**.

The present paper extends the investigations on carbonyl derivatives: amide, thioamide, urea and thiourea complexes of lanthanide $M^{3+}$ cations. Amide binding sites grafted on organized platforms such as calixarenes or resorcinarenes are good cation binders.[21,22] Calixarenes with urea or thiourea functionalized arms have been reported with the main focus on their hydrogen bonding capabilities, leading to supramolecular capsules or calixarene dimers[23] as well as anion complexes in non-aqueous solution.[24,25] Thioamide calixarenes, like acyclic thioamides,[26–29] poorly extract $M^{3+}$ lanthanide cations, compared to their amide analogues and prefer softer transition metals such as $Cu^{2+}$, $Pd^{2+}$, $Cd^{2+}$ or $Ag^{+}$.[30–32]

In this study we compare the ligands (**L**) *N*,*N*′-dimethylacetamide (**A**) and its thioacetamide analogue (**TA**) with tetramethylurea (**U**) and its thiourea analogue (**TU**), shown in Fig. 1. They interact with typical lanthanide cations $M^{3+}$ of decreasing size: $La^{3+}$, $Eu^{3+}$ and $Yb^{3+}$. We first calculated the proton affinities $E_{\mathrm{prot}}$ of the four ligands, as it is generally believed that the proton basicities correlate with cation basicities. We next studied the intrinsic interaction energies $\Delta E$ between **L** and $M^{3+}$, in the absence of other competing species, *i.e.* in the charged $\mathbf{ML}^{3+}$ complexes. Such complexes may poorly model, however, the species formed in condensed phases, where the coordination sphere of the cation is more or less saturated, and hard counterions also often bind to $M^{3+}$. The effect of counterions is thus investigated in the neutral $\mathbf{MCl_3L}$ complexes of 1 : 1 stoichiometry. Moving to higher stoichiometry in the $\mathbf{MCl_3L_2}$ complexes gave further insights into the effect of cumulative ligands in the coordination sphere of $M^{3+}$. For the three type of complexes, we focused on the interaction energies

---

† Tables S1–S3 are available as supplementary data. For direct electronic access see http://www.rsc.org/suppdata/p2/b0/b006585o/

DOI: 10.1039/b006585o

**This journal is © The Royal Society of Chemistry 2001**

**Table 1** Total and relative protonation energies (kcal mol$^{-1}$) from HF/DZ*/HF/DZ* and MP2/DZ*/HF/DZ* calculations without/with BSSE correction

| | HF/DZ*/HF/DZ* | | MP2/DZ*/HF/DZ* | |
|---|---|---|---|---|
| Complex | $\Delta E/\Delta E$cor | $\Delta\Delta E_M/\Delta\Delta E$cor$_M$ | $\Delta E/\Delta E$cor | $\Delta\Delta E_M/\Delta\Delta E$cor$_M$ |
| $(Me_2N)MeCOH^+$ | −226.5/−226.2 | 0.0/0.0 | −220.5/−218.8 | 0.0/0.0 |
| $(Me_2N)MeCSH^+$ | −228.8/−228.6 | −2.3/−2.4 | −222.5/−221.0 | −2.5/−2.2 |
| $(Me_2N)_2COH^+$ | −229.7/−229.4 | −3.2/−3.2 | −225.1/−223.4 | −4.6/−4.6 |
| $(Me_2N)_2CSH^+$ | −232.8/−232.6 | −6.3/−6.4 | −228.1/−226.2 | −7.6/−7.4 |

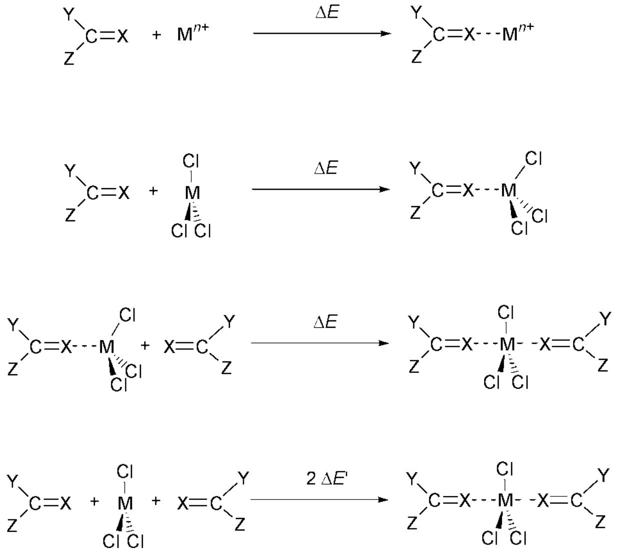

**Fig. 2** Definition of interaction energies $\Delta E$ and $\Delta E'$ (X = O/S; Y, Z = Me/NMe$_2$).

$\Delta E$ between **L** and the other part of the system, as defined in Fig. 2. Structural features of the complexes are also described, as they reveal the stereochemical requirements for ion binding. It will be shown that they are markedly dependent on the type of ligand **L**, as well as on the presence of the other coordinated species (counterions, other ligands). Electronic features of the systems and changes that occur upon complexation will be analysed by the changes in atomic charges.

## Methods

The QM *ab initio* calculations were performed at the HF level using the Gaussian-94 and Gaussian-98 packages.[33,34] We showed that the HF results are comparable with those from MP2 or DFT calculations.[11,14] The 46 + 4f$^n$ core electrons of the lanthanide cations were described by the quasi relativistic pseudopotential of Dolg *et al.*[35,36] and the valence electrons by a (7s,6p,5d)/[5s,4p,3d] Gaussian basis set supplemented by one f polarization function of exponent 0.591, as optimized for La by Frenking *et al.*[37] The H, C, N, O, S and Cl atoms were described by the standard Dunning–Hay double-ζ basis set[38] to which polarization functions (exponents being $\zeta_{3dC} = 0.75$, $\zeta_{3dN} = 0.80$, $\zeta_{3dO} = 0.85$, $\zeta_{3dS} = 0.532$ and $\zeta_{3dCl} = 0.60$) were added.

The geometries of the systems were fully optimized at the HF level using Berny's algorithm without imposing symmetry constraints. Additional tests were performed with the MP2 and B3LYP-DFT methods. The interaction energies of the ligands **L** with $M^{3+}$, $MCl_3$ and $MCl_3$**L** were calculated with respect to the corresponding optimized species. No basis set superposition error ("BSSE") was systematically calculated because the BSSE is nearly constant within a given series.[11,13,14] The atomic charges were obtained by a Mulliken population analysis.

## Results

The total energies of the optimized species are given in Table S1. In this section, we consider, unless otherwise specified, the HF results: interaction energies $\Delta E$ (see Table S2), optimized structural parameters and Mulliken charges (see Table S3). Figs. 3, 4, 6, 9 summarize the main energetic, structural and electronic features for **L**, **LH**$^+$, **ML**$^{3+}$, $MCl_3$ and $MCl_3L_2$ with M = La, Eu and Yb. Some DFT results are presented in the Discussion.

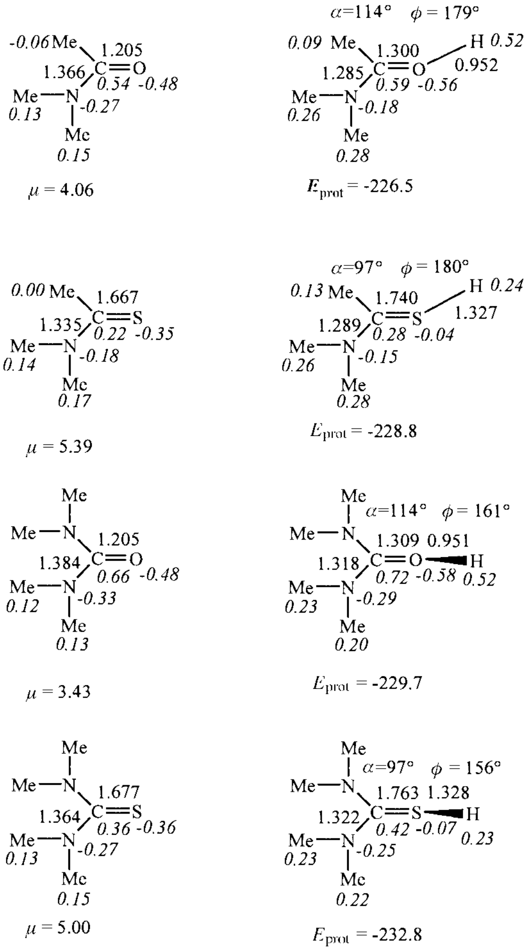

**Fig. 3** Optimized **L** and **LH**$^+$ species: distances (Å), angles (deg) and Mulliken charges (*italics*). Dipole moment of **L** (μ, Debye) and protonation energy ($E_{prot}$, kcal mol$^{-1}$; from HF/DZ*/HF/DZ* calculations without BSSE correction; see also Table 1 for MP2 and BSSE corrected energies).

### 1. The free ligands and their protonation energies

The structures of the optimized ligands **L** and their protonated forms **LH**$^+$ are displayed in Fig. 3. As shown by previous theoretical[39] and experimental results,[40] protonation occurs at oxygen or sulfur, instead of at a nitrogen atom. The calculated protonation energies $E_{prot}$ follow the sequence **TU** > **U** > **TA** > **A**, but the differences are small (6.3 kcal mol$^{-1}$ only along the series). The same sequence has been obtained at higher computational levels and by gas-phase experiments[41] and is confirmed by computations with BSSE correction at the HF level, as well as at the MP2 level (Table 1). Thus, sulfur ligands are somewhat more basic than the oxygen analogues (by 2.3 to 3.1 kcal mol$^{-1}$), and basicities are larger for NMe$_2$ than for Me carbon derivatives (by 3.2 to 4.0 kcal mol$^{-1}$). The higher basicity of sulfur, also observed for other series of compounds (*e.g.* ether/thioether, alcohol/thioalcohols,[42] phosphoryl/thiophosphoryl[14]) relates to its higher polarizability and to the more covalent character of the S–H bond, compared to O–H. Upon protonation, the C=S bond lengthens less (by 0.07 to 0.09 Å) than does the C=O bond (by about 0.10 Å). The greater basicity of sulfur also correlates with the higher dipole moment of **TA** and **TU** (5.4 and 5.0 D, respectively), compared to **A** and **U** (4.1 and 3.4 D, respectively), but not with the Mulliken charges on S/O atoms which yield opposite trends. Another distinct feature concerns the charge transfer $\Delta q$ to the proton, larger (by about 0.3 e) in the sulfur compounds. In the latter, $\Delta q$ stems mostly from the protonated centre (sulfur loses about 0.3 e), while in the oxygen compounds, the oxygen atom becomes more negative (by about 0.1 e) and the charge is transferred from the carbon substituents.

Interesting structural features are noticed in the series. The C=O–H$^+$ angles are comparable in the amide and urea acids (114°), as are the C=S–H$^+$ angles (97°) in the corresponding thio acids. A marked difference is observed between the acetamide **A**H$^+$ and **TA**H$^+$ acids and the urea **U**H$^+$ and **TU**H$^+$ analogues: in the former the proton sits in the plane of the carbonyl or thiocarbonyl groups, while in the latter it is slightly out of plane (the NC–XH dihedral angle is 161° in **U**H$^+$ and 156° in **TU**H$^+$), indicating some repulsion between the proton and the NMe$_2$ groups. Steric hindrance in the urea compounds is also revealed by their non-planarity, leading to almost $C_2$, instead of $C_{2v}$ symmetry (excluding the proton). This non-planarity is consistent with previous studies on unsubstituted urea and thiourea (with NH$_2$, instead of NMe$_2$ groups),[43] as well as for cyclic analogues[44] where the C–N rotational barriers are lower than in the amide analogues.

## 2. The charged 1 : 1 ML$^{3+}$ complexes

According to the calculations, the attraction energies ($-\Delta E$) between the ligands and the lanthanide cations are high (189 to 239 kcal mol$^{-1}$) and decrease in the order **U** > **TU** > **A** > **TA**. Thus, the four ligands bind lanthanide cations as efficiently as Me$_3$P=S and Ph$_3$P=S thiophosphoryl ligands (200 and 230 kcal mol$^{-1}$, respectively), and better than *p*-Me-pyridine (170 kcal mol$^{-1}$).[13] The energy scale in this ligand series is similar (about 20 kcal mol$^{-1}$) for the three cations. This is comparable to the energy difference between H$_2$NMeC=O and Me$_2$NMeC=O acetamide ligands interacting with M$^{3+}$ cations (about 22 kcal mol$^{-1}$)[13] and relatively small, compared to the energy scale in the cation series for a given ligand (from 37 to 40 kcal mol$^{-1}$). For a given ligand, $\Delta E$ increases with the cation hardness (La$^{3+}$ < Eu$^{3+}$ < Yb$^{3+}$), as observed with all **ML**$^{3+}$ systems simulated in similar conditions.[12,13] The $\Delta E$(La, Yb) energy difference, which measures the cation selectivity for a given ligand, follows the same order as the $\Delta E$ values: it is largest for **U** and smallest for **TA** complexes. Thus, sulfur ligands display weaker M$^{3+}$ affinities than oxygen ligands, in contrast to trends in proton affinities. A similarly contrasting trend has been recently reported for R$_3$P=O *vs.* R$_3$P=S ligands.[14] The difference is somewhat larger for amide (8 to 10 kcal mol$^{-1}$ for **A** *vs.* **TA**) than for urea derivatives (6 to 7 kcal mol$^{-1}$ for **U** *vs.* **TU**). Thus, the M$^{3+}$ basicities are more modulated by the Me/NMe$_2$ substitution at carbon than by the S/O substitution. The S/O cation basicity contrasts with observed trends on proton basicities (*vide supra*).

The oxygen/sulfur cation basicity can be qualitatively understood from the HSAB principle, according to which the hard M$^{3+}$ ions prefer the hardest bases, *i.e.* oxygen rather than sulfur ligands, and from the higher electron donation and polarizability of NMe$_2$, compared to Me carbon substituents. There is thus no correlation between the dipole moments of **L** and the $\Delta E$ values (Figs. 3 and 4). The interaction energies $\Delta E$ are markedly dependent on polarization and charge transfer effects, as illustrated by changes in Mulliken charges. The cationic charge ranges from 2.58 (in La**A**$^{3+}$) to 2.11 e (in Yb**TU**$^{3+}$), as the result of electron transfer $\Delta q$ from **L**. For a given ligand, $\Delta q$ increases as $\Delta E$, *i.e.* from La$^{3+}$ to Yb$^{3+}$, but the changes in the cation series are relatively small (0.05 to 0.19 e for a given ligand), compared to the $\Delta q$ in the ligand series (0.24 to 0.42 e for a given cation). The transfer is larger with sulfur than with oxygen compounds (by 0.22 to 0.38 e) and larger for the NMe$_2$ than for the Me carbon substituted ones (by 0.03 to 0.08 e). Thus, the order of M$^{3+}$ basicities does not simply follow the order of the $\Delta q$ values.

The second important effect concerns the polarization of **L** by the cation. We notice that in all **ML**$^{3+}$ complexes the cation sits in the plane of the molecule, which leads to the most effective polarization. In the **U** and **TU** complexes, the cation lies on the C=O or C=S axis, while in the amide **A** and **TA** complexes, it is somewhat *trans* to the C–N bond: the C=O–M angle is 171° with the three cations, while the C=S–M angle ranges from 157° (with Yb) to 161° (with La). The *trans* position is favoured by polarization effects (NR$_2$ is more polarizable than Me) and by steric effects (the Me side is less hindered). Thus, cation coordination is much more linear than proton coordination, due to the different nature of the bonds. As a result of polarization, the $q_O$ or $q_S$ charges are more negative in **ML**$^{3+}$ than in uncomplexed **L**, while the adjacent carbon is more positive. As the S atom transfers more charge to the cation than does the O atom, the charge increase $\Delta q_S$ is smaller than the $\Delta q_O$ increase. As a result of polarization and charge transfer effects, the Me$_N$ and Me$_C$ groups are also more positive in **ML**$^{3+}$ than in **L**.

Concerning the structure of the complexes, we notice that the M–S bonds are about 0.5 Å longer than the M–O ones, while in a cation series, these bonds are shortest with the smallest ion (Yb) and longest with La (by about 0.2 Å). For a given type of binding site (X = O/S), the stronger the interaction energy $\Delta E$, the shorter is the X–M bond: with M = La, the bond variation ranges from 0.02 (X = O) to 0.03 Å (X = S).

The strong electronic perturbations of **L** that occur upon coordination to the cation also translate into large geometry changes: the C=O and C=S bonds lengthen, while the N–C bonds shorten, following trends suggested by the stabilization of the ionic form of the complex (Fig. 5). In the **ML**$^{3+}$ complexes, the C=O and C=S bonds are even longer than in the corresponding protonated C=OH$^+$ and C=SH$^+$ species (see Figs. 3 and 4). They increase in the order La$^{3+}$ < Eu$^{3+}$ < Yb$^{3+}$ in the cation series (by about 0.01 Å) and upon Me→NMe$_2$ carbon substitution (by about 0.01 Å). Thus, compared to the free ligands, the largest deformation $\Delta d$ is observed in the thiourea complex Yb**TU**$^{3+}$ (0.30 Å), while in the corresponding oxygen complex, $\Delta d$ is only 0.18 Å. These deformations again contrast with those observed upon protonation, where C=S was less elongated than C=O. Lanthanide cation coordination results mostly from electrostatic interactions, while protonation involves more covalent binding.

## 3. The neutral MCl$_3$L complexes. Effects of counterions

Addition of a ligand **L** to a neutral MCl$_3$ salt leads to MCl$_3$**L** complexes, where the electrostatic interactions between the MCl$_3$ moiety and **L** are of the dipole–dipole type, and therefore are weaker than the charge–dipole M$^{3+}\cdots$**L** interactions in the **ML**$^{3+}$ complexes. As a result, the interaction energies $\Delta E$ with **L** drop markedly from **ML**$^{3+}$ to MCl$_3$**L** (by a factor of 4.4 to 4.8 for oxygen ligands and 5.4 to 6.1 for sulfur ligands) where $\Delta E$ values range from $-33$ to $-50$ kcal mol$^{-1}$ (Fig. 6). Thus, the preference of oxygen to sulfur ligands (by 8 to 12 kcal mol$^{-1}$) is retained and, in most cases, enhanced in the presence of counterions. On the other hand, the NMe$_2$/Me substituent effect at

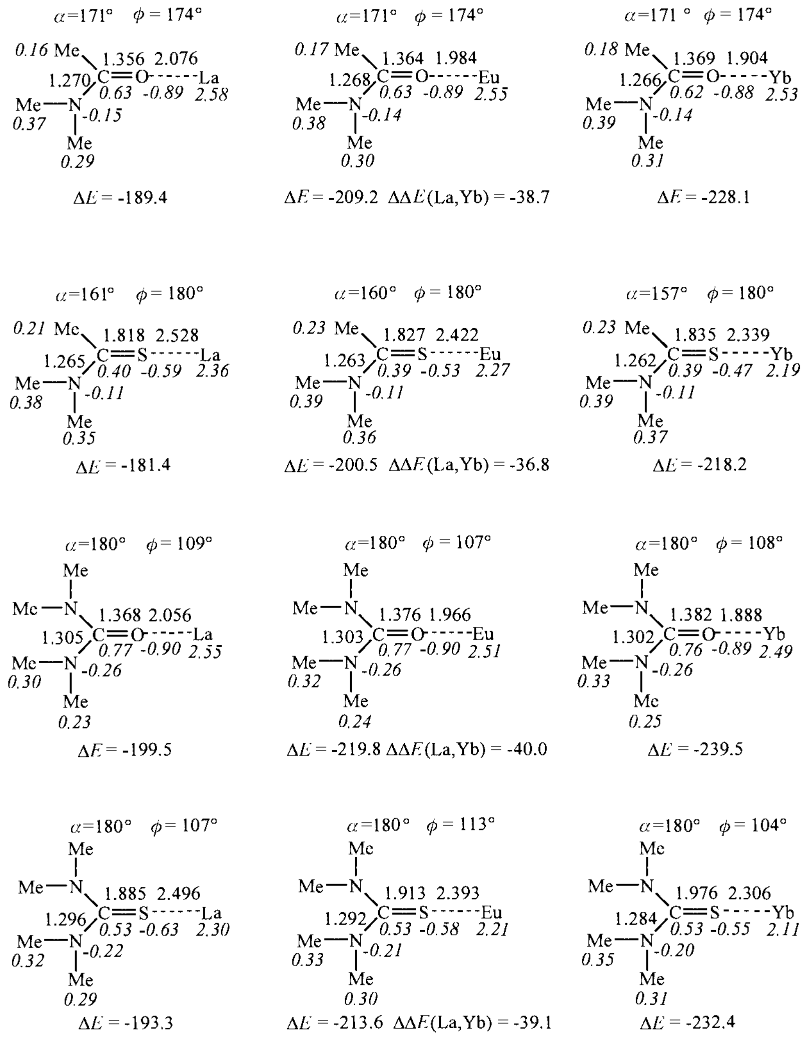

**Fig. 4** Optimized $ML^{3+}$ complexes: distances (Å), angles (deg), Mulliken charges (*italics*). Interaction energies ($\Delta E$, kcal $mol^{-1}$) between $M^{3+}$ and **L** and $\Delta\Delta E$(La, Yb).

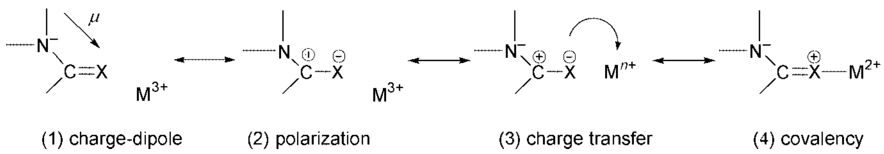

**Fig. 5** Schematic representation of electronic effects in the $ML^{3+}$ complexes.

carbon drops on going from $ML^{3+}$ (14 to 10 kcal $mol^{-1}$) to $MCl_3$**L** complexes (3 to 1 kcal $mol^{-1}$). Thus, in the presence of counterions, the effect of O/S substitution becomes larger than the effect of $NMe_2$/Me carbon substitution, in relation to the different nature of ligand binding in $ML^{3+}$ *vs.* $MCl_3$**L** complexes. As a result, the ligand affinity for a given cation increases in the order **TA** < **TU** < **A** < **U** in $MCl_3$**L** complexes, *i.e.* in a different sequence to the $ML^{3+}$ complexes (**TA** < **A** < **TU** < **U**). We suggest that the **A**/**TU** inversion and the weaker preference for urea, compared to amide derivatives (1–3 kcal $mol^{-1}$ only) are due to destabilizing interactions between the anions and the $NMe_2$ groups in the urea compounds (*vide infra*). These repulsions are antagonistic to the stabilization energy that would result from the larger electron donating capability and polarizability of $NMe_2$ compared to Me.

Adding counterions to the $ML^{3+}$ complexes retains the same order of cation affinities for a given ligand ($La^{3+}$ < $Eu^{3+}$ < $Yb^{3+}$), but the La/Yb binding selectivity $\Delta\Delta E$(La,Yb) drops markedly (from 37–40 kcal $mol^{-1}$ in $ML^{3+}$ to 3–6 kcal $mol^{-1}$ in $MCl_3$**L**). Again, the larger (or smaller) the interaction energy $\Delta E$, the larger (or weaker) is the ion selectivity.

The reduced interactions in $MCl_3$**L**, compared to $ML^{3+}$, translate into larger metal–ligand distances: the S–M bonds lengthen more (by 0.45 to 0.51 Å) than the O–M bonds (by 0.27 to 0.33 Å), and the lengthening increases from Yb to La. The geometry of the ligand is also less perturbed in $MCl_3$**L** than in $ML^{3+}$.

The cation binding mode of **L** is very different in $MCl_3$**L** from that in the $ML^{3+}$ complexes. First, the *α* angle between M with the C=X bond deviates more from linearity. For instance, the C=O–M angle is about 164° in the amide $EuCl_3$**A** complex and 172° in the urea complex **U**$EuCl_3$. In sulfur complexes, the C=S–M angle is 98 to 101°, *i.e.* closer to the value in the protonated $LH^+$ forms than in $ML^{3+}$. Moving from linear to bent coordination is indicative of enhanced covalent binding and of reduced polarization interactions in the $MCl_3$**L** complexes.

The second striking feature concerns the co-planarity of M and the ligands. In one case only ($LaCl_3$**A** complex) the cation sits in the plane of the ligand. In all other cases, it is slightly out of plane, as measured by the *φ* dihedral angles (*φ* = NC–XM; see definition in Fig. 7 and values in Fig. 6). In $EuCl_3$**A** and $YbCl_3$**A**, M is close to the plane of the ligand (*φ* = 160°). This

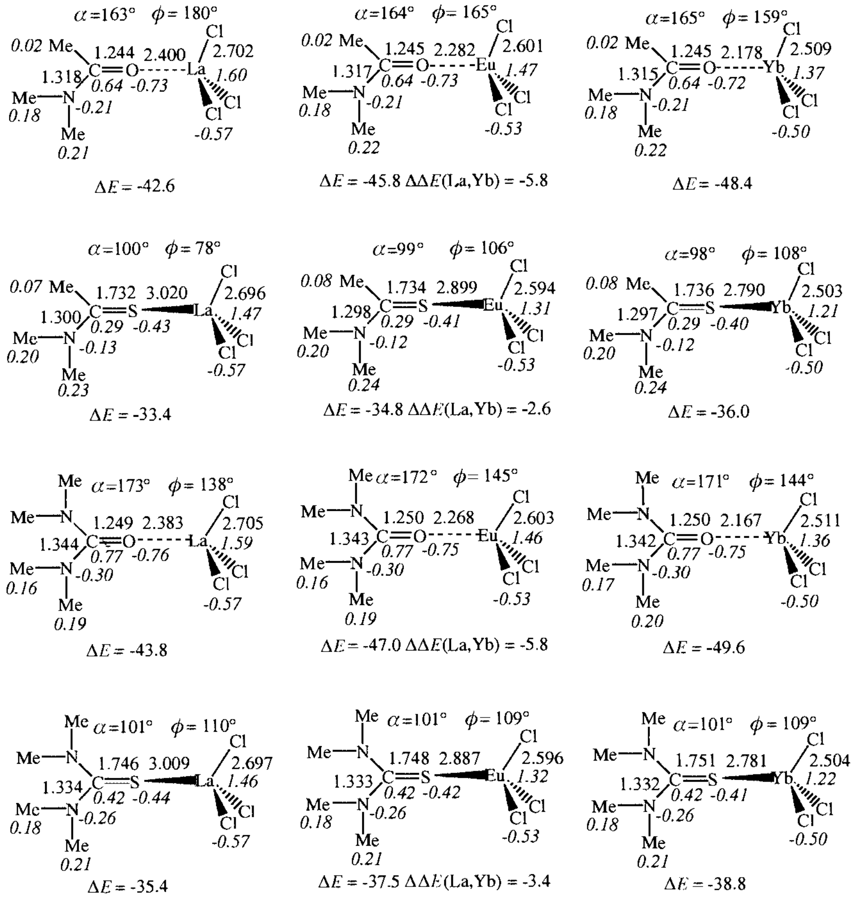

Fig. 6 Optimized $MCl_3L$ complexes: distances (Å), angles (deg), Mulliken charges (*italics*). Interaction energies ($\Delta E$, kcal mol$^{-1}$) between $MCl_3$ and L and $\Delta\Delta E$(La, Yb).

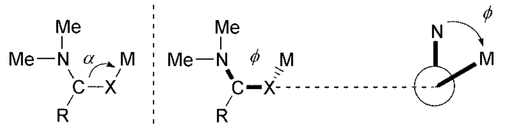

Fig. 7 Definition of non-linear ($\alpha$) and out of plane ($\phi$) cation coordination.

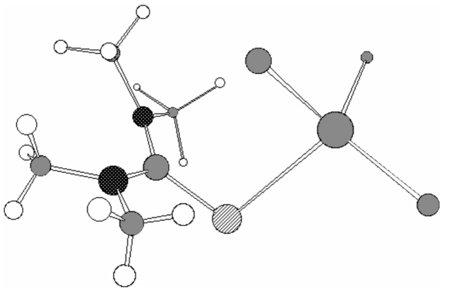

Fig. 8 Structure of the $EuCl_3$**TU** complex.

contrasts with the thioamide analogues $MCl_3$**TA** where the cation sits nearly perpendicular to the plane of the **TA** ligand ($\phi$ ranges from 78 to 108°). Among the urea complexes, non-planarity is again much more pronounced for sulfur complex $MCl_3$**TU** ($\phi = 110°$; see Fig. 8) than for the oxygen $MCl_3$**U** complexes ($\phi = 138$ to 145°). These results suggest that the chloride anions interact repulsively with the ligand, and that the repulsions are larger for the $NMe_2$ than for the Me carbon substituent, and larger for sulfur than for oxygen ligands where the coordination is more linear.

The importance of repulsive interactions between the anions and the amide substituents is supported by the two following "computer experiments". We first optimized the thioformamide (**TFA** = $Me_2NHC{=}S$) $EuCl_3$**TFA** complex, where repulsions between the H atom on the carbon and the anions should be minimal, and found that the Eu atom sits indeed exactly in the plane of **TFA** (the NC–SEu angle is 180°). Furthermore, the binding energy of **TFA** is slightly better (by 0.1 kcal mol$^{-1}$) than the binding of the **TA**, despite the lower polarizability and donating capability of the H atom, compared to the Me group. This is indicative of an intrinsic preference for in-plane binding and of repulsive interactions between the carbon substituent (Me of **TA**, or $NMe_2$ of **U** or **TU**) and the counterions. The second test was run on the thiourea complex $EuCl_3$**TU**, which was optimized with the Eu atom respectively "in-plane" (NC–SEu angle constrained at 0°) and "perpendicular to the plane" of the ligand (NC–SEu angle constrained at 90°). The "in plane" binding turns out to be 6.7 kcal mol$^{-1}$ less stable than the "perpendicular" binding. The corresponding C=S–Eu angle is more open for the planar binding (129°) than for the "perpendicular" binding (102°), also indicating larger repulsions in the former. The out-of-plane metal binding to sulfur ligands is also observed in solid state structures of analogous complexes (*vide infra*).

The Mulliken charges also reveal the difference in ligand binding to $MCl_3$, compared to $M^{3+}$. We first notice that, in relation to the electron donation from the anions to the metal (0.50 to 0.43 e per chloride), the metal charge is much less positive (1.6 to 1.2 e) in the $MCl_3$**L** than in **ML**$^{3+}$ complexes. The $MCl_3$ moiety is pyramidal (the X–M–Cl angle ranges from 99 to 103°), leading to a dipole which interacts with the **L** ligand much less than does the "naked" $M^{3+}$ cation. As a result, the charge transfer from **L** drops from **ML**$^{3+}$ (0.42–0.89 e) to $MCl_3$**L** (0.11–0.29 e). It is larger for sulfur than for oxygen ligands (0.15 e) and similar for $NMe_2$ and Me substituted

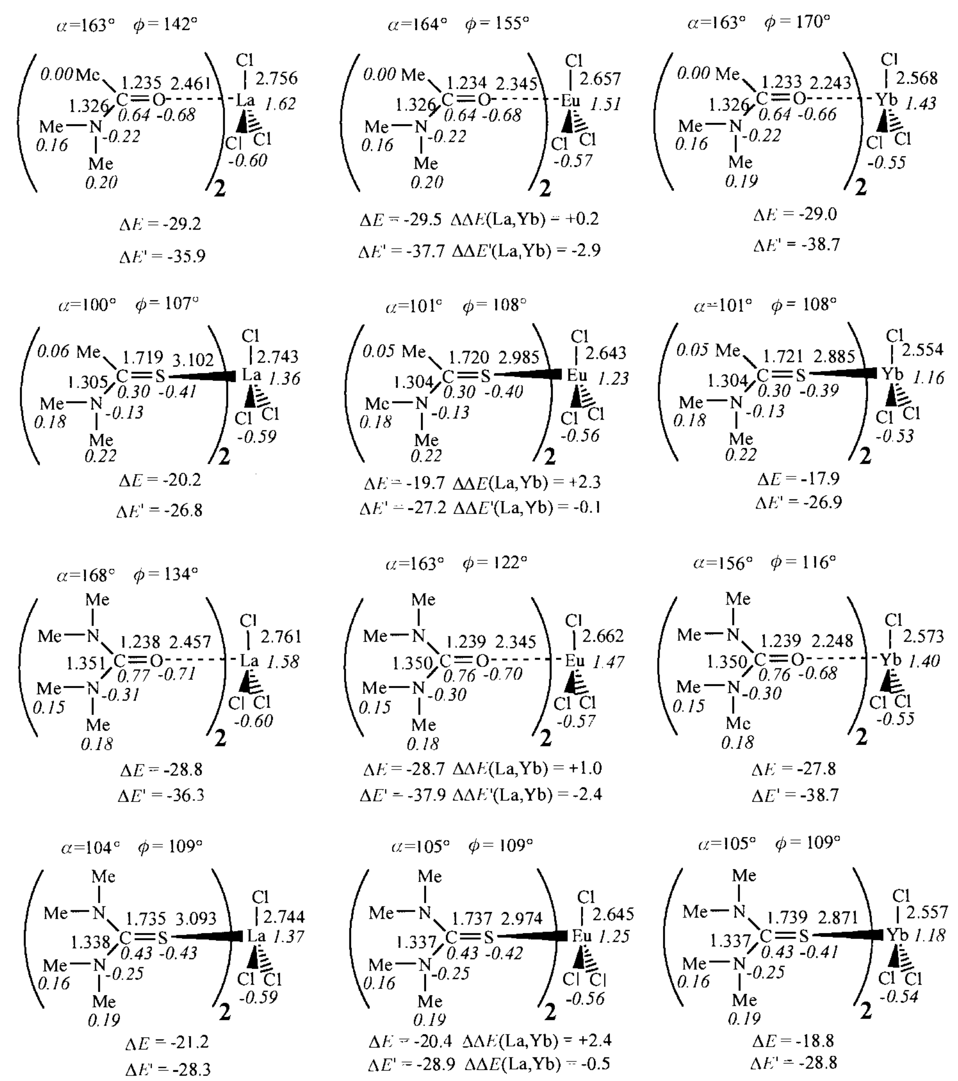

**Fig. 9** Optimized $MCl_3L_2$ complexes: distances (Å), angles (deg), Mulliken charges (*italics*). Interaction energies ($\Delta E$, kcal $mol^{-1}$) between $MCl_3$**L** and **L**, $\Delta E'$ and $\Delta\Delta E$(La, Yb).

carbon. Also, the charge of the coordinated atoms (X = O/S) lies between the charge in $MCl_3$**L** and uncomplexed **L**, due to the reduced contribution of polarization effects.

## 4. Neutral $MCl_3L_2$ complexes

Adding a second ligand to the $MCl_3$**L** complex leads to a coordination number of five, closer to the coordination in condensed media. The corresponding binding energy $\Delta E$ has been compared to the average binding energy *per ligand* $\Delta E'$ (Table S2 and Fig. 9), $\Delta E'$ being somewhat larger than $\Delta E$ (by 7 to 11 kcal $mol^{-1}$). We first discuss the $\Delta E$ binding energy, which ranges from 18 to 29 kcal $mol^{-1}$ for all $MCl_3L_2$ complexes. The drop in $\Delta E$ from the first to the second ligand is more pronounced for oxygen (65%) than for sulfur compounds (55%) and for the Yb cation, which is complexed best by all the ligands in the $ML^{3+}$ and $MCl_3$**L** series. This leads to a levelling of all $\Delta E$ values and to inversions compared to the $MCl_3$**L** complexes. With the four ligands, the $\Delta\Delta E$(La,Yb) difference becomes positive (from 0.5 to 2.4 kcal $mol^{-1}$), which means that **L** binds better to the lanthanum than to the ytterbium for the $MCl_3$**L** complexes. We suggest that this inversion stems from "strain repulsion" in the first coordination sphere of the cation, which is antagonistic to the metal–ligand and metal–anion attractions. These repulsions are most effective with the smallest cation Yb. Thus, the order of metal affinities is Yb < Eu < La for the **TA**, **U** and **TU** ligands. With the **A** ligand, the $\Delta\Delta E$(La,Yb) is smallest (0.5 kcal $mol^{-1}$) and europium is slightly preferred (Yb < La < Eu). Thus, *increasing the coordination number of the metal does not simply scale down the ligand binding energies, but modulates the order of ion discrimination for a given ligand.* For a given metal, the preference for oxygen *vs.* sulfur ligands is retained (by about 10 kcal $mol^{-1}$) and the ligands bind in the order **TA** < **TU** < **U** < **A**. The **A**/**U** order is thus different from the order in the $MCl_3$**L** complexes, but in both cases, the differences $\Delta\Delta E$(**A**, **U**) and $\Delta\Delta E$(**TA**, **TU**) are small (about 1 kcal $mol^{-1}$).

Looking at the $\Delta E'$ average interaction energy *per ligand* yields similar conclusions to the $\Delta E$ energies, as far as the comparison of ligands for a given metal is concerned (Fig. 9). The **U**/**A** order is inversed but the difference in $\Delta E$ as well as in $\Delta E'$ values is small (from 0.0 to 1.2 kcal $mol^{-1}$). The order in the cation series for a given **L** also differs somewhat. In most cases, binding to ytterbium is preferred over lanthanum, but the difference is small (from 0.1 to 2.9 kcal $mol^{-1}$). This is because the $\Delta E'$ energies lie between the $\Delta E$ values in $MCl_3L_2$ and in $MCl_3$**L**, and contain therefore relatively more attraction (which favour Yb) than repulsion (which favour La) contributions.

Some features may also be noticed concerning the structure of $MCl_3L_2$ complexes. Although no symmetry was imposed during the minimization, the two optimized ligands are related by a $C_2$ symmetry axis and the $MCl_3$ moiety is planar. The zero dipole moment of $MCl_3$ explains, in addition to the ligand–ligand repulsions, the weaker binding of **L**. As a result, the metal–ligand distances are longer in $MCl_3L_2$ than in $MCl_3$**L** (by 0.06 to 0.08 Å with oxygen ligands and by 0.08–0.09 Å with sulfur ligands). The ligand structures are also less perturbed than in $MCl_3$**L**: the C=O and C=S bonds are shorter, and the C–N bonds are longer (by about 0.01 Å), being much closer to the structures of uncomplexed **L**. The cation binding mode is very close to that found in $MCl_3$**L** complexes. In the oxygen complexes, the C=O–M angles are almost linear (156 to 168°) and the cation sits closer to the plane of the amide **A** ($\phi$ = 142 to 170°) than in the case of the urea **U** ligand ($\phi$ = 116 to 134°). In the sulfur complexes, the C=S–M angles are bent (100 to 105°) and the cation sits nearly perpendicular to the plane of the ligands ($\phi$ = 107 to 109°).

The trends in Mulliken charges in the cation series, as well as in the ligand series, remain the same in $MCl_3$**L**$_2$ as in the $MCl_3$**L** series. The electron transfer per ligand is larger with sulfur (0.20 to 0.23 e) than with oxygen (0.09 to 0.13 e) ligands, and larger with $NMe_2$ than with Me carbon substituents. This is slightly less than in $MCl_3$**L** complexes. Notice also that electron donation from the chloride ions is smaller in $MCl_3$**L**$_2$ than in $MCl_3$**L** and smaller with oxygen than with sulfur ligands. As a result, the metal charge is reduced upon addition of a second ligand to the sulfur complexes, but increased for oxygen complexes.

## Discussion and conclusion

We report consistent calculations on the lanthanide complexes of two important classes of carbonyl ligands, amide and urea, respectively, and of their thio analogues. When compared to other ligands such as pyridine derivatives, anisole and phosphoryl compounds,[12,13] the results show that these molecules are good ligands for trivalent lanthanide cations.

### Proton *vs.* cation affinity of the ligands

Comparison with protonation energies allows one to gain insights into possible correlations between the ligand proton basicities and cation basicities. We notice that correlations are generally indirectly inferred from measurements involving weak interactions in solution with Lewis acids (*e.g.* with $SbCl_5$ or $I_2$[20,45]) or with hydrogen bonded molecules. Concerning the amide/thioamide comparison, the hydrogen bonding formation constants in $CCl_4$ solution are larger for the former ligands,[46,47] as supported by theoretical investigations on related systems.[48,49] This order of hydrogen bonding contrasts with the order of protonation energies calculated by us and by others,[47] according to which thio compounds are preferred. Generally speaking, proton basicities involve major electronic perturbations of the ligand and may not correlate with hydrogen bonding which leads to minor perturbations only.

The next stage is to consider the ligand affinities for hard cations. As shown by experiments on gas-phase lithium basicities,[50,51] fair correlations with proton affinities can be observed for homogeneous classes of ligands, but correlations involving different classes are less good. Our calculations show that *the interactions with lanthanide cations are markedly modulated by the presence of counterions and by the stoichiometry*. Intrinsically, for **ML**$^{3+}$ complexes, the cation prefers the harder oxygen ligands to their sulfur analogues, following an opposite trend to the proton basicities. The difference stems from the less covalent character of the metal–ligand bond compared with the proton–ligand bond, and from marked polarization effects in **ML**$^{3+}$. As counterions are added to the system, the ligand formally binds to a neutral $MCl_3$ salt, leading to reduced interactions. This leads to an amplification of the sulfur/oxygen discrimination, and a reduction of substituent effects at carbon. The order of cation affinities is the same in both **ML**$^{3+}$ and $MCl_3$**L** complexes, following the ion hardness ($Yb^{3+} > Eu^{3+} > La^{3+}$).

The relative interactions of sulfur *vs.* oxygen ligands with "acids" $A$ ($A = H^+$, $M^{3+}$, $MCl_3$) can be assessed *via* the isodesmic reaction shown in Fig. 10 where X = Me *vs.* $NMe_2$. The results (Table 2) confirm that the proton prefers the softer sulfur ligands, while the $M^{3+}$ and $MCl_3$ "acids" prefer the harder oxygen ligands, the effect being more pronounced with the amide **A** (X = Me) than with the urea **U** (X = $NMe_2$) ligands. This observation is also more pronounced with $MCl_3$ than with the $M^{3+}$ acid, due to more repulsive interactions between the counterions and the sulfur ligands. Thus, *counterions and cumulative interactions in the first coordination sphere of the cation play an important role in ion discrimination by a given ligand, as well as on ligand recognition by a given ion.* As shown by recent NMR studies on calixarene–CMPO derivatives, the nature of the lanthanide complexes also depends on the presence of competing binders such as polar solvent molecules, or hard anions.[52] Our calculations demonstrate how counterions modulate the nature of metal–ligand bonds and lead to a reversal of ion binding affinities: the intrinsically preferred $Yb^{3+}$ cation is less well bound in the presence of counterions and other ligands than the sterically more accessible $La^{3+}$ cation.

**Fig. 10** Isodesmic reaction used to compare the interaction of "acids" ($A = H^+$, $M^{3+}$, $MCl_3$) with oxygen *vs.* sulfur "bases".

**Table 2** Energies $E_{iso}$ (kcal mol$^{-1}$) of the isodesmic reaction (XMe)-C=O + (XMe)C=S-$A$→(XMe)C=O-$A$ + (XMe)C=S

| | | Acid $A$ | | | | | | |
|---|---|---|---|---|---|---|---|---|
| X | Y | $H^+$ | $La^{3+}$ | $Eu^{3+}$ | $Yb^{3+}$ | $LaCl_3$ | $EuCl_3$ | $YbCl_3$ |
| Me | $NMe_2$ | 2.3 | −8.0 | −8.7 | −9.9 | −9.2 | −11.0 | −12.4 |
| $NMe_2$ | $NMe_2$ | 3.1 | −6.2 | −6.2 | −7.1 | −8.4 | −9.5 | −10.8 |

### Structural features of the complexes

Counterions and stoichiometry also change the structure of the coordinated ligand, which is less perturbed in $MCl_3$**L** and $MCl_3$**L**$_2$ than in the **ML**$^{3+}$ complexes, where polarization effects are magnified. Thus, comparisons with solid state structures or with structures in condensed phases should be done with the most saturated (here, $MCl_3$**L**$_2$) species. We previously discussed the structure of acetamide complexes, showing good agreement between calculated and X-ray structures.[13] A review of amide complexation can be found in ref. 53 and typical features of **A** and **U** complexes are reported in Table 3. We notice that in most solid state structures, the anions are directly coordinated to the metal, and the C=O–M angles are bent. One exception concerns the $M(ClO_4)_3$**U**$_6$ complexes (M = Er; Yb) where this angle is linear as in the optimized **MU**$^{3+}$ species. Experimental results on $Yb(ClO_4)_3$**U**$_6$ at different temperatures also reveal thermal effects on bond lengths (the Yb–O distance ranges from 2.18 Å at −158 °C to 2.13 Å at 70 °C). The calculated structures of $LaCl_3$**A** and of $YbCl_3$**A** agree within 0.03–0.05 Å with the X-ray structures of the corresponding La and Yb complexes. The experimental structures of the Sm and Er complexes of **A** are also close to those optimized for the corresponding (and similar in size) metals Eu and Yb.

Consideration of other amide complexes of the cations under study retrieved from the Cambridge Crystallographic Database reveals some disparity between the experimental M–O distances, and general agreement with the optimized distances in $MCl_3$**L**$_2$. This is observed for M = La (25 structures, La–O = 2.39–2.61 Å; average = 2.50 Å, to be compared with the optimized distance of 2.46 Å), M = Eu (17 structures, Eu–O = 2.31–2.51 Å, average = 2.40 Å; optimized value is 2.35 Å)

**Table 3** Structural features of complexes of **A** and **U** in the solid state (retrieved from the Cambridge Crystallographic Database)[67]

| Refcode | Formula | CN | M···O/Å | O=C/Å | α/deg | ϕ/deg | Ref. |
|---|---|---|---|---|---|---|---|
| CAXYIJ | $La((^iPrO)_2PS_2)_3\mathbf{A}_2$ | 8 | 2.41–2.43 | 1.21–1.26 | 144–166 | 99–113 | 68 |
| CIDJUU | $Sm(NO_3)_3\mathbf{A}_3$ | 9 | 2.31–2.32 | 1.21–1.27 | 140–155 | 116–175 | 69 |
| CIDKAB | $Er(NO_3)_3\mathbf{A}_3$ | 9 | 2.24–2.29 | 1.23–1.31 | 140–163 | 111–156 | 69 |
| JAQCIN[a] | $Yb(Ni(CN)_4)Cl\mathbf{A}_4$ | 7 | 2.20–2.27 | 1.27–1.33 | 133–160 | 121–145 | 70 |
| LELBOT | $Ce(C_5H_5)_3\mathbf{U}$ | 4 | 2.46 | 1.26 | 155 | 97 | 71 |
| WEHTOS | $Ce(picrate)_3\mathbf{U}_3$ | 6 | 2.37–2.42 | 1.22–1.26 | 143–172 | 98–104 | 72 |
| LELBUZ | $Nd(C_5H_5)_3\mathbf{U}$ | 4 | 2.44 | 1.26 | 154 | 100 | 71 |
| WEHTUY | $Nd(picrate)_3\mathbf{U}_3$ | 6 | 2.36–2.40 | 1.23–1.25 | 142–158 | 96–106 | 72 |
| TMUNEU | $Eu(NO_3)_3\mathbf{U}_3$ | 9 | 2.30–2.35 | 1.23–1.27 | 143–170 | 98–118 | 73 |
| HURERC | $Er(ClO_4)_3\mathbf{U}_6$ | 6 | 2.18–2.20 | 1.27–1.30 | 178–179 | 95–114 | 74 |
| VITTIB | $Yb(ClO_4)_3\mathbf{U}_6$ | 6 | 2.17 | 1.27 | 177 | 142 | 75 |

[a] X-Ray structure at −60 °C.

and M = Yb (6 structures; Yb–O = 2.24–2.46 Å; average = 2.30 Å; calculated value is 2.24 Å). Similar features are found for urea complexes with Eu or Yb, or the related Ce (close to La), Nd (close to Eu) or Er (close to Yb) analogues.

For the sulfur compounds, no solid state structure could be found that can be directly compared with the calculated ones. For instance, in the $Gd^{3+}$ and $Sm^{3+}$ complexes of **TU**, the ligands are bidentate (*via* S and N atoms) and achieve bridging coordination to two cations.[54] The corresponding M–S distances (2.94 and 3.06 Å) are close to the optimized Eu–S distance of 2.97 Å. Structures of lanthanide complexes of negatively charged dithiocarbamate $RR'NCS_2^-$ ligands have also been reported,[55,56] but the metal–ligand distances are shorter than with the neutral **TA** or **TU** ligands (by 0.12 Å with M = La and 0.17 Å with M = Yb), in accord with the stronger attractions to the metal.

Another interesting aspect of metal binding concerns the co-planarity of the cation with the ligand. The planar binding in $\mathbf{ML}^{3+}$ complexes contrasts with the out-of-plane binding, especially with sulfur ligands in the presence of counterions. According to a recent review,[53] out-of-plane binding is not uncommon for amide ligands and is shown by our calculations to be induced by other coordinated species. Out-of-plane coordination is most pronounced with thiourea **TU**, in accord with the more bent C=S–M angle, which also leads to enhanced repulsions between the anions and the $NMe_2$ urea substituents. Although no structure was found for similar lanthanide complexes, a number of thiourea halide complexes with such a deformation have been reported, with M = Sb ($\phi$ = 94–114°),[57–59] Os ($\phi$ = 94–97°),[60] Re ($\phi$ = 101–143°),[61,62] Ru ($\phi$ = 94°),[63] Pt ($\phi$ = 114°),[64] Zn ($\phi$ = 119–150°)[65] and Hg ($\phi$ = 99–159°).[66] Noteworthy are the soft character of these metals and the presence of coordinated (generally halide) counterions. There are structures, however (M = Cu, Au, W, Mo, Rh), where the metal is more co-planar with thioamide or thiourea ligands ($\phi > 160°$). According to our study, *out-of-plane binding is not an intrinsic feature of the metal–thiourea bond, but results from avoiding repulsions in the planar binding mode*. We suggest that monitoring the stereochemistry of metal–ligand interactions *via* preorganized arrangements of the latter (*e.g.* on calixarene or resorcinarene platforms) might lead to ion discrimination by oxygen/sulfur binding sites. The binding mode of counterions clearly contributes to that process.

### Computational aspects

Concerning the computations, we previously found that the conclusions obtained on similar amide, phosphoryl and pyridine lanthanide complexes from HF calculations are validated by MP2 and B3LYP-DFT calculations.[11,13–15] We decided however to reoptimize the four $EuCl_3\mathbf{L}$ complexes to compare the interaction energies $\Delta E$ and structures. It can be seen from Table 4 that the HF *vs.* DFT $\Delta E$ values differ by at most 1.4 kcal mol$^{-1}$ and the order of the ligand binding sequence is identical. Table 4 also confirms that BSSE corrections at the HF or DFT level are relatively small and nearly constant, yielding nearly identical differences in binding energies $\Delta E$. HF *vs.* DFT optimized distances differ by 0.01 to 0.03 Å. The Eu···**L** and Eu–Cl distances are somewhat shorter and the C=O and C=S bonds are longer in the DFT optimized structures, but the structural trends are the same with both methods (Table 5). Trends concerning the non-linearity of the C=X–M angles are also similar ($\alpha$ angles differ by 2 to 12°). In the DFT structures the cation is somewhat more out of the plane of the ligands ($\phi$ angles differ by 3 to 35°), and this non-planarity is more pronounced with the sulfur compounds, as found in the HF calculations and in the solid state structures. Another issue concerns the representation of the lanthanide cations, where it would be desirable to compare the large core ECPs used here to small core ones. In the case of the $Eu^{3+}\cdots O{=}PH_3$ complex, the two types of representations were found to lead to similar results,[10] but this question remains to be more systematically investigated.

**Table 4** Comparison of HF *vs.* DFT interaction energies $\Delta E$ (kcal mol$^{-1}$) in $EuCl_3\mathbf{L}$ complexes. $\Delta\Delta E_M$ are the differences in $\Delta E$, relative to the $\mathbf{A}EuCl_3$ complex. Uncorrected/BSSE corrected energies

| Complex | $\Delta E/\Delta E_{cor}$ | $\Delta\Delta E_M/\Delta E_{corM}$ |
|---|---|---|
| HF/DZ*//HF/DZ* | | |
| $(Me_2N)MeCO\cdots EuCl_3$ | −45.8/−43.2 | 0.0/0.0 |
| $(Me_2N)MeCS\cdots EuCl_3$ | −34.8/−31.3 | +11.0/+11.9 |
| $(Me_2N)_2CO\cdots EuCl_3$ | −47.0/−44.5 | −1.2/−1.3 |
| $(Me_2N)_2CS\cdots EuCl_3$ | −37.5/−34.0 | +8.3/+9.2 |
| DFT/DZ*//DFT/DZ* | | |
| $(Me_2N)MeCO\cdots EuCl_3$ | −44.4/−40.3 | 0.0/0.0 |
| $(Me_2N)MeCS\cdots EuCl_3$ | −33.5/−29.8 | +10.9/+10.5 |
| $(Me_2N)_2CO\cdots EuCl_3$ | −46.8/−42.6 | −2.4/−2.3 |
| $(Me_2N)_2CS\cdots EuCl_3$ | −37.9/−33.9 | +6.5/+6.4 |

To conclude, we emphasize the importance of computational approaches to study cation complexes of increasing complexity and to compare the intrinsic binding features of various classes of ligands used in the complexation and liquid–liquid extraction of lanthanide and actinide cations. Such computations should contribute to a better understanding of the structural and energetic features of the complexes and the basis of efficient complexation and separation of lanthanides and actinides by known or putative ligands.

## Acknowledgements

The authors are grateful to EEC (FIKW-CT-2000-0088) and PRACTIS for support, and to IDRIS and Université Louis Pasteur for allocation of computer resources. F. B. is grateful to the French ministry of Research for a grant.

**Table 5** Comparison of HF *vs.* DFT optimized structures and Mulliken charges $q$ of **L** and EuCl$_3$**L** complexes

| | M–X/Å | C–X/Å | M–Cl/Å | $\alpha$/deg | $\phi$/deg | X–M–Cl/deg | $q$(M) | $q$(X) | $q$(C) | $q$(Cl) |
|---|---|---|---|---|---|---|---|---|---|---|
| HF/DZ* | | | | | | | | | | |
| (Me$_2$N)MeCO | — | 1.205 | — | — | — | — | — | −0.48 | 0.54 | — |
| (Me$_2$N)MeCS | — | 1.667 | — | — | — | — | — | −0.35 | 0.22 | — |
| (Me$_2$N)$_2$CO | — | 1.205 | — | — | — | — | — | −0.48 | 0.66 | — |
| (Me$_2$N)$_2$CS | — | 1.677 | — | — | — | — | — | −0.36 | 0.36 | — |
| (Me$_2$N)MeCO···EuCl$_3$ | 2.282 | 1.245 | 2.601 | 164 | 165 | 100 | 1.47 | −0.73 | 0.64 | −0.53 |
| (Me$_2$N)MeCS···EuCl$_3$ | 2.899 | 1.734 | 2.594 | 99 | 106 | 102 | 1.31 | −0.41 | 0.29 | −0.53 |
| (Me$_2$N)$_2$CO···EuCl$_3$ | 2.268 | 1.250 | 2.603 | 172 | 145 | 101 | 1.46 | −0.75 | 0.77 | −0.53 |
| (Me$_2$N)$_2$CS···EuCl$_3$ | 2.887 | 1.748 | 2.596 | 101 | 109 | 102 | 1.32 | −0.42 | 0.42 | −0.53 |
| DFT/DZ* | | | | | | | | | | |
| (Me$_2$N)MeCO | — | 1.233 | — | — | — | — | — | −0.35 | 0.29 | — |
| (Me$_2$N)MeCS | — | 1.675 | — | — | — | — | — | −0.25 | 0.05 | — |
| (Me$_2$N)$_2$CO | — | 1.233 | — | — | — | — | — | −0.35 | 0.31 | — |
| (Me$_2$N)$_2$CS | — | 1.684 | — | — | — | — | — | −0.27 | 0.07 | — |
| (Me$_2$N)MeCO···EuCl$_3$ | 2.264 | 1.266 | 2.570 | 162 | 130 | 101 | 1.04 | −0.49 | 0.39 | −0.42 |
| (Me$_2$N)MeCS···EuCl$_3$ | 2.851 | 1.731 | 2.563 | 96 | 100 | 103 | 0.91 | −0.28 | 0.11 | −0.42 |
| (Me$_2$N)$_2$CO···EuCl$_3$ | 2.252 | 1.274 | 2.574 | 160 | 130 | 101 | 1.02 | −0.51 | 0.39 | −0.42 |
| (Me$_2$N)$_2$CS···EuCl$_3$ | 2.839 | 1.747 | 2.567 | 99 | 112 | 103 | 0.91 | −0.29 | 0.10 | −0.42 |

## References

1 V. Alexander, *Chem. Rev.*, 1995, **95**, 273.

2 L. Cecille, M. Casarci and L. Pietrelli, *New Separation Chemistry Techniques for Radioactive Waste and Other Specific Applications*, 1991, Commission of the European Communities, Elsevier Applied Science, London, New York.

3 G. R. Choppin and K. L. Nash, *Radiochim. Acta*, 1995, **70/71**, 225.

4 G. R. Choppin and D. R. Peterman, *Coord. Chem. Rev.*, 1998, **174**, 283.

5 N. Sabbatini, A. Mecati, M. Guardigli, V. Balzani, J. M. Lehn, R. Ziessel and R. Ungaro, *J. Lumin.*, 1991, **48–49**, 463.

6 W. D. J. Horrocks and D. R. Sudnik, *J. Am. Chem. Soc.*, 1979, **101**, 334.

7 D. Parker and J. A. G. Williams, *J. Chem. Soc.*, *Dalton Trans.*, 1996, 3613.

8 J. M. Lehn, *Struct. Bonding* (*Berlin*), 1973, **161**, 1.

9 F. Hutschka, L. Troxler, A. Dedieu and G. Wipff, *J. Phys. Chem. A*, 1998, **102**, 3773.

10 L. Troxler, A. Dedieu, F. Hutschka and G. Wipff, *THEOCHEM*, 1998, **431**, 151.

11 R. Schurhammer, V. Erhart, L. Troxler and G. Wipff, *J. Chem. Soc.*, *Perkin Trans. 2*, 1999, 2515.

12 M. Baaden, F. Berny, C. Boehme, N. Muzet, R. Schurhammer and G. Wipff, *J. Alloys Compd.*, 2000, **303–304**, 104.

13 F. Berny, N. Muzet, L. Troxler, A. Dedieu and G. Wipff, *Inorg. Chem.*, 1999, **38**, 1244.

14 C. Boehme and G. Wipff, *J. Phys. Chem. A*, 1999, **103**, 6023.

15 C. Boehme and G. Wipff, *Inorg. Chem.*, 1999, **38**, 5734.

16 J. Chen, Y. Zhu and R. Jiao, *Sep. Sci. Technol.*, 1996, **31**, 2724.

17 C. Hill, C. Madic, P. Baron, M. Ozawa and Y. Tanaka, *J. Alloys Compd.*, 1998, **271–273**, 159.

18 R. G. Pearson, *Hard and Soft Acids and Bases*, Dowdon, Hutchinson and Ross Publ., Stroudsburg, PA, 1973.

19 G. R. Choppin, in *Principles of Solvent Extraction*, ed. J. Rydberg, C. Musikas and G. R. Choppin, M. Dekker, New York, pp. 71–100, 1992.

20 R. D. Hancock and A. E. Martell, *Chem. Rev.*, 1989, **89**, 1875, and references cited therein.

21 F. Arnaud-Neu, S. Barboso, F. Berny, A. Casnati, N. Muzet, A. Pinalli, R. Ungaro, M.-J. Schwing-Weill and G. Wipff, *J. Chem. Soc.*, *Perkin Trans. 2*, 1999, 1727.

22 A. M. Kervey, M.-J. Schwing-Weill and F. Arnaud-Neu, in *Comprehensive Supramolecular Chemistry*, ed. J. L. Atwood, J. E. D. Davies, D. D. McNicol, F. Vögtle and J.-M. Lehn, Pergamon, New York, 1996, pp. 537–603.

23 J. J. Gonzales, R. Ferdani, E. Albertini, J. M. Blasco, A. Arduini, A. Pochini, P. Prados and J. de Mendoza, *Chem. Eur. J.*, 2000, **6**, 73.

24 J. W. M. Nissink, H. Boerrigter, W. Verboom, D. N. Reinhoudt and J. H. van der Maas, *J. Chem. Soc.*, *Perkin Trans. 2*, 1998, 2623.

25 H. Boerrigter, L. Grave, J. W. M. Nissink, L. A. J. Chrisstoffels, J. H. van der Maas, W. Verboom, F. de Jong and D. N. Reinhoudt, *J. Org. Chem.*, 1998, **63**, 4174.

26 F. Z. El Aamrani, A. Kumar and A. M. Sastre, *New J. Chem.*, 1999, **23**, 517.

27 A. Ceresa and E. Pretsch, *Anal. Chim. Acta*, 1999, **395**, 41.

28 T. Kowalik-Jankowska, M. Jasionowski, L. Lankiewicz and H. Kozlowski, *J. Inorg. Biochem.*, 1997, 45.

29 J. S. Kim, M. H. Cho, J. H. Cho, J. H. Lee, R. A. Bartsch, Y. I. Lee and I. H. Kim, *Talanta*, 2000, **51**, 99.

30 R. J. W. Lugtenberg, R. J. M. Egberink, J. F. J. Engbersen and D. N. Reinhoudt, *J. Chem. Soc.*, *Perkin Trans. 2*, 1997, 1353.

31 F. Arnaud-Neu, G. Barrett, D. Corry, S. Cremin, G. Ferguson, J. F. Gallagher, S. J. Harris, M. A. McKervey and M.-J. Schwing-Weill, *J. Chem. Soc.*, *Perkin Trans. 2*, 1997, 575.

32 W. Wroblewski and Z. Brzozka, *Anal. Chim. Acta*, 1996, **326**, 163.

33 M. J. Frisch, G. W. Trucks, H. B. Schlegel, P. M. W. Gill, B. G. Johnson, M. A. Robb, J. R. Cheeseman, T. Keith, G. A. Petersson, J. A. Montgomery, K. Raghavachari, M. A. Al-Laham, V. G. Zakrzewski, J. V. Ortiz, J. B. Foresman, C. Y. Peng, P. Y. Ayala, W. Chen, M. W. Wong, J. L. Andres, E. S. Replogle, R. Gomperts, R. L. Martin, D. J. Fox, J. S. Binkley, D. J. Defrees, J. Baker, J. P. Stewart, M. Head-Gordon, C. Gonzalez and J. A. Pople, *Gaussian 94, Revision B.2*, Gaussian, Inc., Pittsburgh, PA, 1995.

34 M. J. Frisch, G. W. Trucks, H. B. Schlegel, G. E. Scuseria, M. A. Robb, J. R. Cheeseman, V. G. Zakrzewski, J. A. Montgomery Jr., R. E. Stratmann, J. C. Burant, S. Dapprich, J. M. Millam, A. D. Daniels, K. N. Kudin, M. C. Strain, O. Farkas, J. Tomasi, V. Barone, M. Cossi, R. Cammi, B. Mennucci, C. Pomelli, C. Adamo, S. Clifford, J. Ochterski, G. A. Petersson, P. Y. Ayala, Q. Cui, K. Morokuma, D. K. Malick, A. D. Rabuck, K. Raghavachari, J. B. Foresman, J. Cioslowski, J. V. Ortiz, B. B. Stefanov, G. Liu, A. Liashenko, P. Piskorz, I. Komaromi, R. Gomperts, R. L. Martin, D. J. Fox, T. Keith, M. A. Al-Laham, C. Y. Peng, A. Nanayakkara, C. Gonzalez, M. Challacombe, P. M. W. Gill, B. Johnson, W. Chen, M. W. Wong, J. L. Andres, M. Head-Gordon, E. S. Replogle and J. A. Pople, *Gaussian 98, Revision A.5*, Gaussian, Inc., Pittsburgh, PA, 1998.

35 M. Dolg, H. Stoll and H. Preuss, *J. Chem. Phys.*, 1989, **90**, 1730.

36 M. Dolg, H. Stoll, A. Savin and H. Preuss, *Theor. Chim. Acta*, 1993, **85**, 441.

37 A. W. Ehlers, M. Böhme, S. Dapprich, A. Gobbi, A. Höllwarth, V. Jonas, K. F. Köhler, R. Stegmann, A. Veldkamp and G. Frenking, *Chem. Phys. Lett.*, 1993, **208**, 111.

38 T. H. Dunning and P. J. Hay, in *Methods of Electronic Structure Theory. Modern Theoretical Chemistry 3*, ed. H. F. Schaefer III, Plenum Press, New York, 1977, pp. 1–28.

39 F. Wang, S. Ma, D. Zhang and R. G. Cooks, *J. Phys. Chem. A*, 1998, **102**, 2988.

40 G. A. Olah, A. Burrichter, G. Rasul, K. O. Christe and G. K. S. Prakash, *J. Am. Chem. Soc.*, 1997, **119**, 4345.

41 J.-L. M. Abboud, A. Mo, J. L. G. de Paz, M. Yanez, M. Esseffar, W. Bouab, M. El-Mouhtadi, R. Mikhlisse, E. Ballesteros, M. Herreros, H. Homan, C. Lopez-Mardomingo and R. Notario, *J. Am. Chem. Soc.*, 1993, **115**, 12468.

42 P. Kebarle, *Annu. Rev. Phys. Chem.*, 1977, **28**, 445.

43 W. Kim, H.-J. Lee, Y. S. Choi, J.-H. Choi and C.-J. Yoon, *J. Chem. Soc., Faraday Trans.*, 1998, **94**, 2663.
44 E. Kleinpeter, *J. Mol. Struct.*, 1996, **380**, 139.
45 V. Gutman, *The Donor–Acceptor Approach to Molecular Interactions*, Plenum Press, New York, 1980.
46 C. Laurence, M. Berthelot, Y. J. Le Questel and M. L. El Ghomari, *J. Chem. Soc., Perkin Trans. 2*, 1995, 2075, and references cited therein.
47 B. K. Min, H.-J. Lee, Y. S. Choi, J. Park, C.-J. Yoon and J.-A. Yu, *THEOCHEM*, 1998, **471**, 283.
48 R. J. Boyd, *THEOCHEM*, 1985, **133**, 45.
49 A. Masunov and J. J. Dannenberg, *J. Phys. Chem. B*, 2000, **104**, 806.
50 P. Burk, I. A. Koppel, I. Koppel, R. Kurg, J.-F. Gal, P.-C. Maria, M. Herreros, R. Notario, J.-L. M. Abboud, F. Anvia and R. W. Taft, *J. Phys. Chem. A*, 2000, 2824.
51 R. W. Taft, F. Anvia, J.-F. Gal, S. Walsh, M. Capon, M. C. Holmes, K. Hosn, G. Oloumi, R. Vasanwala and S. Yazdani, *Pure Appl. Chem.*, 1990, **62**, 17.
52 B. Lambert, V. Jacques, A. Shivanyuk, S. E. Matthews, A. Tunayar, M. Baaden, G. Wipff, V. Böhmer and J.-F. Desreux, *Inorg. Chem.*, 2000, **39**, 2033.
53 O. Clement, B. M. Rapko and B. P. Hay, *Coord. Chem. Rev.*, 1998, **170**, 203.
54 M. Geissinger and J. Magull, *Z. Anorg. Allg. Chem.*, 1996, **622**, 734.
55 T. D. Tilley, R. A. Andersen, A. Zalkin and D. H. Templeton, *Inorg. Chem.*, 1982, **21**, 2644.
56 H. Jinshun, L. Shanhuo, W. Manfang, Z. Qianer and L. Jiaxi, *Wuji Huaxue Xuebao* (*J. Inorg. Chem.*), 1987, **3**, 1.
57 B. Rubin, F. J. Heldrich, W. K. Dean, D. J. Williams and A. Viehbeck, *Inorg. Chem.*, 1981, **20**, 4434.
58 E. Hough and D. G. Nicholson, *J. Chem. Soc., Dalton Trans.*, 1981, 2083.
59 P. Berges, W. Hinrichs, J. Kopf, D. Mandak and G. Klar, *J. Chem. Res.*, 1985.
60 T. Lis and P. Starynowicz, *Acta Crystallogr., Sect. C*, 1985, **41**, 1299.
61 T. Lis, *Acta Crystallogr., Sect. B*, 1976, **32**, 2707.
62 T. Lis, *Acta Crystallogr., Sect. B*, 1977, **33**, 944.
63 D. P. Fairlie, W. A. Wickramasinghe, K. A. Byriel and H. Taube, *Inorg. Chem.*, 1997, **36**, 2242.
64 U. Bierbach, T. W. Hambley, J. D. Roberts and N. Farrell, *Inorg. Chem.*, 1996, **35**, 4865.
65 I. Potocnak, M. Dunaj-Jurco, V. Petricek and J. Cernak, *Acta Crystallogr., Sect. C*, 1994, **50**, 1902.
66 M. Cannas, F. A. Devillanova, G. Marongiu and G. Verani, *J. Inorg. Nucl. Chem.*, 1981, **43**, 2383.
67 F. Allen and O. Kennard, *Chem. Des. Autom. News*, 1993, **8**, 31.
68 K. Nagai, Y. Sato, S. Kondo and A. Ouchi, *Bull. Chem. Soc. Jpn.*, 1983, **56**, 2605.
69 M. D. Matheus, J. L. Brianso, X. Solans, G. Germain and J. P. Declercq, *Z. Kristallogr.*, 1983, **165**, 233.
70 D. W. Knoeppel, J. Liu, E. A. Meyers and S. G. Shore, *Inorg. Chem.*, 1998, **37**, 4828.
71 A. Domingos, N. Marques, A. P. D. Matos, M. G. Silva-Valenzuela and L. B. Zinner, *Polyhedron*, 1993, **12**, 2545.
72 C. Barberato and E. Castellano, *Acta Crystallogr., Sect. C*, 1994, **50**, 351.
73 C. Chieh, G. E. Toogood, T. D. Boyle and C. M. Burgess, *Acta Crystallogr., Sect. B*, 1976, **32**, 1008.
74 L. A. Aslanov, V. M. Ionov and S. S. Sotman, *Kristallografiya*, 1976, **21**, 1200.
75 T. Y. Lyubeznova, V. I. Ponomarev and L. A. Aslanov, *Kristallografiya*, 1990, **35**, 746.